Available online at www.sciencedirect.com
ScienceDirect
Journal of Power Sources 162 (2006) 597–605
JOURNAL OF POWER SOURCES
www.elsevier.com/locate/jpowsour

A reforming system for co-generation of hydrogen and mechanical work from methanol

Maxim Lyubovsky *, Dennis Walsh [1]

Precision Combustion, Inc., 410 Sackett Point Road, North Haven, CT 06473, United States

Received 2 June 2006; received in revised form 17 July 2006; accepted 18 July 2006
Available online 18 September 2006

Abstract

The paper describes a reforming system for converting methanol into pure hydrogen. The system is based on an autothermal reforming reactor operating at elevated pressures followed by membrane-based hydrogen separation. The high-pressure membrane retentate stream is combusted and expanded through a turbine generating additional power. Process simulation illustrates the effects of the system operating parameters on performance and demonstrates system reforming efficiency up to ~90%. When coupled with a PEM fuel cell and an electrical generator, overall fuel to electricity efficiency can be >48% depending upon the efficiency of a PEM fuel cell stack.

Keywords: Autothermal reforming; Hydrogen; Fuel cell; Renewable power

1. Introduction

To satisfy long-term world energy demands, practical alternatives to traditional fossil fuels will need to be identified and implemented. Long-term energy solutions likely will include solar and/or nuclear based power cycles. Practical utilization of both energy sources requires energy carriers that allow efficient accumulation, transportation and storage of energy and are readily suitable to the end user.

Hydrogen is broadly considered as an energy intermediate of the future that can be utilized in either fuel cell or more traditional combustion based power systems. While hydrogen can be efficiently produced from natural gas or other hydrocarbons in large industrial reformers, transporting and storing hydrogen poses significant challenges due to its gaseous state and very low volumetric power density. This places hydrogen at a disadvantage as an energy carrier for distributed and mobile applications. The ideal carrier should be liquid under the normal climate conditions, should have high power density and should be able to be efficiently converted into electricity or mechanical power at the end user's site.

Methanol and ethanol satisfy these requirements and are readily available in large quantities. Although, the energy density of alcohols is about half that for gasoline or diesel, alcohols are more reactive and can be reformed into hydrogen in a relatively low temperature process, thus relaxing requirements to the reforming system. Methanol can be produced from natural gas through a so-called gas-to-methanol (GTM) process as means of bringing stranded natural gas to the markets. Ethanol can be produced by fermentation of biomass, i.e. a renewable energy resource. Alcohol based power systems, therefore, can contribute to the transition from fossil to renewable energy sources.

Alcohols can be converted into hydrogen through steam reforming [1–3] or autothermal reforming [4–7] processes. Selection between these two approaches depends on the details of the reformer integration into the fuel processing system and an assessment of overall system efficiency, size and complexity. Lattner and Harold [8] provided modeling and comparative analysis for three different methanol processing systems, based on steam reforming (SR), autothermal reforming (ATR), and ATR membrane reactors. The models suggest that all systems can achieve about 50% efficiency, while the ATR-membrane based system can be much smaller in size. All the systems considered were relatively complex, incorporating multiple heat exchange and stream conditioning elements.

* Corresponding author. Present address: H2Gen Innovations, Inc., 4740 Eisenhower Ave., Alexandria, VA 22304, United States.
Tel.: +1 703 212 7444x249; fax: +1 703 212 4898.
E-mail address: mlyubovs@h2gen.com (M. Lyubovsky).
[1] Consultant to PCI.

0378-7753/$ – see front matter © 2006 Elsevier B.V. All rights reserved.
doi:10.1016/j.jpowsour.2006.07.035

In this paper, we demonstrate a model for a fuel processing system converting alcohol fuel into hydrogen and mechanical work. Simulations are run assuming methanol as fuel. It is expected, though, that a system operating on ethanol would show similar characteristics [7]. The system is based on an autothermal reforming reactor operating at elevated pressures followed by membrane-based hydrogen separation. The high-pressure membrane discharge stream is combusted and expanded through a turbine generating additional power. Only one heat exchanger is required in the system to recover heat from the turbine exhaust stream for vaporization of methanol and water feeds to the ATR. We use process simulation modeling based on our previous experimental data on autothermal reforming (oxidative steam reforming) of methanol and literature data for hydrogen separation membrane performance to illustrate the effect of the system operating parameters on performance.

2. Thermodynamic analysis of the methanol processing system

The fuel processing system analyzed in this paper is designed to produce pure hydrogen gas, i.e. to convert methanol into H_2 and CO_2 in a series of chemical reactions and/or separation steps. Any CO formed in the primary reformer would be removed either by its conversion into CO_2 in downstream processing, such as water-gas-shift (WGS) and preferential oxidation (PROX) and/or by hydrogen separation through a membrane or a pressure swing adsorption (PSA) unit, followed by CO combustion. Lumped reforming processes, therefore, can be represented by Eq. (1) below, where the coefficients for the required water and oxygen are adjusted to provide an overall thermally neutral reaction.

$$\mathrm{CH_3OH(l)} + 0.54\,\mathrm{H_2O(l)} + 0.23\,\mathrm{O_2} \rightarrow \mathrm{CO_2} + 2.54\,\mathrm{H_2}\ \Delta H = 0\,\mathrm{kJ\,mol^{-1}} \quad (1)$$

Eq. (1) represents an *ideal* reforming process, where methanol is completely converted into hydrogen and CO_2 and no heat is lost. Note, that methanol and water are liquids at ambient conditions. Heat required for vaporization of these components is taken into account in Eq. (1). Eq. (1) shows the maximum amount of hydrogen, which can be produced in any type of a reforming process if no external heat import is available. This maximum value is independent of the reforming strategy and provides a means for comparing different reforming systems on the basis of hydrogen output per unit of reformed fuel. Note that this maximum hydrogen output exactly corresponds to 100% efficiency based on higher heating values (HHV) of methanol and hydrogen given by Eq. (2) below.

$$\eta = 100\% \times \frac{\mathrm{HHV(H_2)}}{\mathrm{HHV(CH_3OH)}} \quad (2)$$

Eq. (1) also shows the *ideal* amounts of oxygen and water required for converting methanol into hydrogen with 100% efficiency. Additional oxygen leads to net heat release in the system. Additional water consumes unrecoverable heat for vaporization. Increasing the O:C and S:C ratios above that are shown in Eq. (1), which is always the case for operating a real reforming system, would result in lost heat, lower hydrogen yield and decreased system efficiency.

The above analysis corresponds to an ideal, lumped reforming process in which H_2 and CO_2 are the only products. In actual autothermal reforming of methanol, however, some CO will be formed in addition to CO_2. Also fuel, oxygen and water may not be fully consumed. Increasing the air added to the mixture drives the reaction increasingly in the direction of complete combustion with resultant increases in the adiabatic equilibrium temperature and decreases in hydrogen yield. Methane and other components may form as by-products, especially at higher operating temperatures. This suggests that preferably the process should be operated with the lowest practical amount of air in the feed mixture.

Thermodynamic analysis of the ATR process with varying feed mixtures predicts low concentrations of CO. For example, departing from the maximum hydrogen production conditions of Eq. (1) above, a feed having O:C∼0.24 and S:C∼1 has a predicted equilibrium CO yield of only ∼1.4%. Increasing inlet steam content can further reduce CO formation with attendant impact on process efficiency for reasons noted above.

3. Reforming system model

The general approach to a reforming system for converting methanol into hydrogen is similar to the system described in our previous work [9] for reforming of methane. The systems are based on an ATR reformer operating at elevated pressures followed by a membrane based hydrogen separator, a membrane retentate burner and a turbine for mechanical power recovery. Details of system integration and description of the assumptions used in modeling of individual components for the described system was provided in [9]. The difference between this and our previous work is based on the fact that methanol can be converted to CO and H_2 at much lower temperatures than methane, which allows combining reforming and water-gas-shift steps within a single reactor [6]. Reformate temperature for such an ATR reactor can be compatible with a Pd-based membrane, such that no stream conditioning between these process elements would be required. Such a reforming reactor requires addition of steam to the inlet mixture, unlike the methane reforming system described previously [9], where dry catalytic partial oxidation reactor (CPOX) was used to convert methane into syngas and water was added between the CPOX and the WGS reactors and used to cool the flow. Also for the methanol system, heat contained in the turbine exhaust stream can be used to vaporize and pre-heat the methanol and water ATR feeds. In this work, system modeling was performed using ASPEN^{TM} simulation software to develop the representations of the proposed reforming system shown in Fig. 1.

Table 1 summarizes the conditions and assumptions for each case modeled in this study. A total of seven cases of system operation were studied in which system parameters and assumptions about the system performance were modified as described below. Fig. 1A shows the model bases case for the reforming

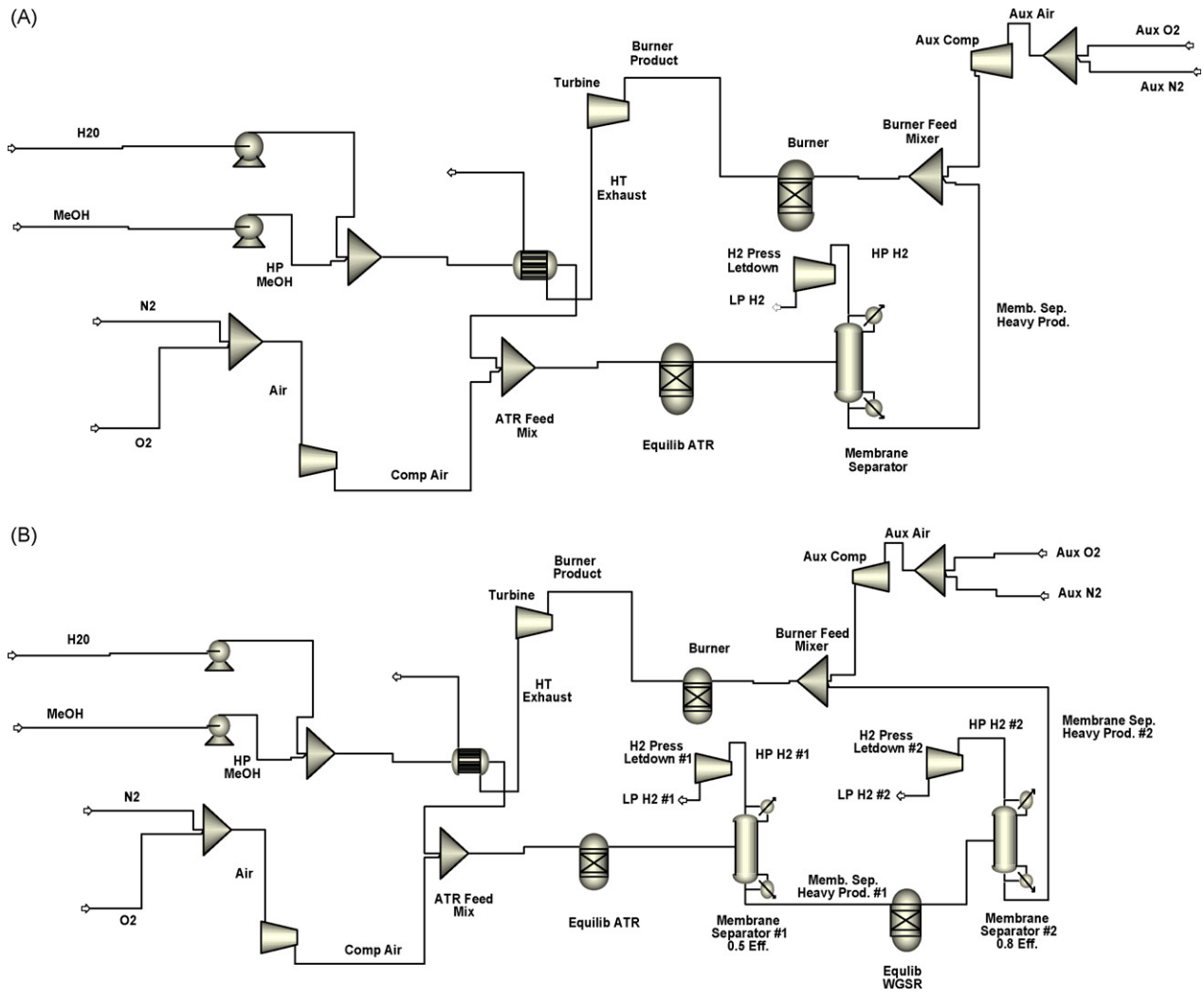

Fig. 1. Schematic representation of the methanol reforming system used for modeling the system performance. (A) Base case with no WGS activity in the membrane unit and (B) assumption of WGS reaction in the membrane unit.

system, while the Fig. 1B shows the same system in which WGS activity is assumed in the Pd based membrane separator unit.

In all cases studied, pure methanol was considered as the fuel. Methanol was mixed with water at 1:1 molar ratio before feeding the mixture to the boiler heat exchanger. The work for pumping liquid methanol and water to the operating pressure is neglected. In a real system, alcohol and water can be mixed at low pressure such that only one pump could be used.

Table 1
Summary of conditions and assumptions for modeled cases

Case #	Pressure (atm)	ATR exit T	CH_4	Burner air	WGS in membrane
1	15	500	NO	ER = 1.2	No
2	15	450	NO	ER = 1.2	No
3	15	450	NO	T = 1150	No
4	15	450	0.2%	ER = 1.2	No
5	15	450	0.2%	T = 1150	No
6	15	450	0.2%	T = 1150	Yes
7	5	450	0.2%	T = 1150	Yes

Air is represented as a mixture of 21% O_2 and 79% N_2 at ambient conditions (pressure and temperature). As a convenience in the model, separate compressors are shown for the reformer and the combustor air streams, though in practice a single compressor may be used with a controlled air split between the two streams. Both compressors are assumed to have efficiencies of 87% relative to isentropic. Air, methanol and steam are assumed to be perfectly mixed before entering the ATR reactor.

Autothermal reforming of alcohols into hydrogen has been demonstrated by many researchers [4–7]. In our previous work, complete conversion of methanol in adiabatic ATR reactor was demonstrated with near equilibrium product composition and about 50% H_2 and less than 2% CO in the reformate stream [6]. The product composition and temperature for this reactor depended on the inlet mixture temperature, oxygen-to-carbon (O:C) and steam-to-carbon (S:C) ratios. In this study, the ATR reactor was modeled as an equilibrium adiabatic reactor operating at the system pressure. The air-to-fuel ratio was adjusted to achieve a specified temperature at the ATR exit (either 450 or 500 °C). At these low ATR temperatures, very high concentrations are predicted for methane by thermody-

namic analysis if methane is included as an allowed equilibrium product. Experimentally, though, it was observed that, while some methane is usually formed in the ATR and WGS reactors, the concentration is typically small. This suggests that the influence of the undesired methanation reaction can be minimized by employing catalysts that kinetically suppress this reaction. To study the effect of methanation on the overall system performance, in some of the studied cases methane formation was completely prohibited, while in alternative cases methane formation producing a fixed 0.2 mol.% concentration in the reformate stream was specified (this level is consistent with the results of our previous work [6]). Methane is then considered inert in the membrane separation unit and is combusted in the retentate burner together with CO and unseparated H_2. Because of the ATR's low operating temperature, no separate WGS reactor is included in the model. Reformate exiting the ATR is directly fed into the membrane separation unit.

The membrane unit is assumed to segregate pure hydrogen at ambient pressure from the high-pressure reformate mixture produced by the ATR reactor. In the model shown in Fig. 1A, the membrane separation is represented as a two step process involving a flow split at constant system pressure in which a specified amount of hydrogen is segregated from the reformate stream followed by a pressure let-down which reduces the pressure of the high purity hydrogen stream to atmospheric (no credit is taken for the work performed by the H_2 expander since it is only a modeling convenience—not an actual process unit). The amount of hydrogen removed by the separator is calculated assuming a fractional approach to the partial pressure equilibrium between the pure hydrogen stream and the separator exhaust stream according to the equation.

$$\eta P_{\text{sys}} \frac{(n-x)}{(f-x)} = 1\,\text{atm}, \tag{3}$$

where η is the approach to thermodynamic equilibrium, P_{sys} the system pressure, f the total molar flow, n the molar flow of H_2 at the separator inlet and x is the molar flow of H_2 at the pure hydrogen stream separator unit at 1 atm pressure. Eq. (3) assumes that at the exit of the separator unit partial pressure of hydrogen on the reformate side of the membrane (given by a ratio of hydrogen flow $(n-x)$ to a total flow $(f-x)$ at system pressure P_{sys}, where x is the flow of hydrogen across the membrane) remains higher than ambient pressure of pure hydrogen on the permeate side by a factor $1/\eta$. In all cases described here (except the case 6, were lower values for η had to be used), 80% approach to equilibrium separation ($\eta = 0.8$) was assumed.

This separator model assumes that the membrane is catalytically inert and only removes hydrogen from the reformate stream. In practice, a Pd based membrane may provide sufficient catalytic activity to support the WGS reaction. As hydrogen is removed from the mixture, WGS equilibrium is shifted resulting in further conversion of CO into additional hydrogen along the membrane. In the system shown in Fig. 1B, a membrane having WGS activity is modeled as a series of two membrane separators having an adiabatic equilibrium WGS reactor between them. Each membrane performs catalytically inert hydrogen separation at some specified approach to thermodynamic equilibrium.

The separator discharge stream which remains at the system pressure is mixed with air and is completely oxidized in an adiabatic, equilibrium burner. The excess air supplied to the burner is either controlled at 1.2 times the stoichiometric amount required to oxidize all burnable components in the discharge stream to CO_2 and H_2O or the amount of air is adjusted to provide a set temperature at the burner exit. In our study, the burner exit temperature for these cases was selected at 1150 °C, which is below the material limits for the components of most modern gas turbines.

The burner discharge stream is expanded from the system operating pressure to atmospheric pressure through a gas turbine to produce mechanical work. A turbine efficiency of 89% is assumed relative to isentropic. The turbine exhaust stream, which is at ambient pressure, is passed through the heat exchanger to vaporize methanol and water feeds to ATR. The heat exchanger duty is sufficient to vaporize all components of the inlet stream with the hot side temperature remaining above the liquid vaporization temperature.

Table 2
Flow components and power loads for the methanol reforming system (Case #1)

	ATR air compressor	ATR inlet	ATR exit	H_2 output	Burner air compressor	Burner inlet	Burner exit	Turbine exit
CH_3OH (mol h^{-1})	0	1000	0	0	0	0	0	0
CH_4 (mol h^{-1})	0	0	0	0	0	0	0	0
O_2 (mol h^{-1})	243	243	0	0	353	353	59	59
N_2(mol h^{-1})	913	913	913	0	1329	2242	2242	2242
H_2O (mol h^{-1})	0	1000	825	0	0	825	1074	1074
CO (mol h^{-1})	0	0	340	0	0	340	0	0
CO_2 (mol h^{-1})	0	0	660	0	0	660	1000	1000
H_2 (mol h^{-1})	0	0	2175	1926	0	249	0	0
Total flow (mol h^{-1})	1156	3156	4913	1926	1682	4669	4375	4375
Temperature (°C)	412	224	500		412	472	1348	749
Pressure (atm)	15	15	15	1	15	15	15	1
Heating value (kW)	0.0	212.0	199.2	152.8	0.0	46.5	0.0	0.0
Mechanical work (kW)	−3.78				−5.43			30.74

Table 3
Flow components and power loads for the methanol reforming system (Case #2)

	ATR air compressor	ATR inlet	ATR exit	H_2 output	Burner air compressor	Burner inlet	Burner exit	Turbine exit
CH_3OH (mol h^{-1})	0	1000	0	0	0	0	0	0
CH_4 (mol h^{-1})	0	0	0	0	0	0	0	0
O_2 (mol h^{-1})	222	222	0	0	313	313	52	52
N_2 (mol h^{-1})	834	834	834	0	1177	2011	2011	2011
H_2O (mol h^{-1})	0	1000	732	0	0	732	965	965
CO (mol h^{-1})	0	0	288	0	0	288	0	0
CO_2 (mol h^{-1})	0	0	712	0	0	712	1000	1000
H_2 (mol h^{-1})	0	0	2268	2035	0	233	0	0
Total flow (mol h^{-1})	1056	3056	4834	2035	1490	4289	4028	4028
Temperature (°C)	412	219	450		412	438	1278	706
Pressure (atm)	15	15	15	1	15	15	15	1
Heating value (kW)	0.0	212.0	202.5	161.4	0.0	41.1	0.0	0.0
Mechanical work (kW)	−3.40				−4.80			26.96

Table 4
Flow components and power loads for the methanol reforming system (Case #3)

	ATR air compressor	ATR inlet	ATR exit	H_2 output	burner air compressor	burner inlet	burner exit	turbine exit
CH_3OH (mol h^{-1})	0	1000	0	0	0	0	0	0
CH_4 (mol h^{-1})	0	0	0	0	0	0	0	0
O_2 (mol h^{-1})	222	222	0	0	506	506	245	245
N_2 (mol h^{-1})	834	834	834	0	1903	2737	2737	2737
H_2O (mol h^{-1})	0	1000	732	0	0	732	965	965
CO (mol h^{-1})	0	0	288	0	0	288	0	0
CO_2 (mol h^{-1})	0	0	712	0	0	712	1000	1000
H_2 (mol h^{-1})	0	0	2268	2035	0	233	0	0
Total flow (mol h^{-1})	1056	3056	4834	2035	2409	5208	4947	4947
Temperature (°C)	412	219	450		412	434	1149	602
Pressure (atm)	15	15	15	1	15	15	15	1
Heating value (kW)	0.0	212.0	202.5	161.4	0.0	41.1	0.0	0.0
Mechanical work (kW)	−3.40				−7.78			30.09

4. Results and discussion

4.1. System efficiency

Results for the system simulations for cases 1–7 are shown in Tables 2–8. For all studies methanol feed to the system is chosen arbitrarily at 1 kmol h^{-1}. This corresponds to ∼202 kW_t thermal input based on the higher heating value (HHV) of liquid methanol supplied to the system. Flows for all other streams and operating conditions for system components shown in Tables 2–8 are based on the methanol input and are calculated using the relationships described above. The tables show gas composition and temperature at different points along the system, as well as the power loads for the system components.

Table 5
Flow components and power loads for the methanol reforming system (Case #4)

	ATR air compressor	ATR inlet	ATR exit	H_2 output	Burner air compressor	Burner inlet	Burner exit	Turbine exit
CH_3OH (mol h^{-1})	0	1000	0	0	0	0	0	0
CH_4 (mol h^{-1})	0	0	9.7	0	0	9.7	0	
O_2 (mol h^{-1})	217	217	0	0	332	332	55	55
N_2 (mol h^{-1})	818	818	818	0	1249	2067	2067	2067
H_2O (mol h^{-1})	0	1000	737	0	0	737	988	988
CO (mol h^{-1})	0	0	282	0	0	282	0	0
CO_2 (mol h^{-1})	0	0	708	0	0	708	1000	1000
H_2 (mol h^{-1})	0	0	2244	2012	0	232	0	0
Total flow (mol h^{-1})	1035	3035	4799	2012	1581	4368	4110	4110
Temperature (°C)	412	218	450		412	438	1296	717
Pressure (atm)	15	15	15	1	15	15	15	1
Heating value (kW)	0.0	212.0	202.6	159.6	0.0	42.9	0.0	0.0
Mechanical work (kW)	−3.34				−5.10			27.90

Table 6
Flow components and power loads for the methanol reforming system (Case #5)

	ATR air compressor	ATR inlet	ATR exit	H_2 output	Burner air compressor	Burner inlet	Burner exit	Turbine exit
CH_3OH (mol h^{-1})	0	1000	0	0	0	0	0	0
CH_4 (mol h^{-1})	0	0	9.7	0	0	9.7	0	
O_2 (mol h^{-1})	217	217	0	0	556	556	279	279
N_2 (mol h^{-1})	818	818	818	0	2091	2909	2909	2909
H_2O (mol h^{-1})	0	1000	737	0	0	737	988	988
CO (mol h^{-1})	0	0	282	0	0	282	0	0
CO_2 (mol h^{-1})	0	0	708	0	0	708	1000	1000
H_2 (mol h^{-1})	0	0	2244	2012	0	232	0	0
Total flow (mol h^{-1})	1035	3035	4799	2012	2647	5434	5176	5176
Temperature (°C)	412	218	450		412	433	1149	599
Pressure (atm)	15	15	15	1	15	15	15	1
Heating value (kW)	0.0	212.0	202.6	159.6	0.0	42.9	0.0	0.0
Mechanical work (kW)	−3.34				−8.53			31.38

Table 7
Flow components and power loads for the methanol reforming system (Case #6)

	ATR air compressor	ATR inlet	ATR exit	H_2 output	Burner air compressor	Burner inlet	Burner exit	Turbine exit
CH_3OH (mol h^{-1})	0	1000	0	0	0	0	0	0
CH_4 (mol h^{-1})	0	0	9.7	0	0	9.7	0	
O_2 (mol h^{-1})	217	217	0	0	524	524	255	255
N_2 (mol h^{-1})	818	818	818	0	1972	2790	2790	2790
H_2O (mol h^{-1})	0	1000	737	0	0	598	973	973
CO (mol h^{-1})	0	0	282	0	0	143	0	0
CO_2 (mol h^{-1})	0	0	708	0	0	847	1000	1000
H_2 (mol h^{-1})	0	0	2244	2028	0	355	0	0
Total flow (mol h^{-1})	1035	3035	4799	2028	2496	5267	5018	5018
Temperature (°C)	412	218	450		412	461	1149	601
Pressure (atm)	15	15	15	1	15	15	15	1
Heating value (kW)	0.0	212.0	202.6	160.9	0.0	41.8	0.0	0.0
Mechanical work (kW)	−3.34				−8.06			30.45

In the ATR inlet calculations shown in Tables 2–8, methanol is considered in vaporized state, therefore, the heating value increased to 212.0 kW.

Power load and efficiency calculations for all the cases are also summarized in Table 9. Hydrogen yield efficiency is calculated as the ratio of the HHV of the H_2 recovered from the membrane separator unit to the HHV of liquid methanol supplied to the system. (Note that the heat required for vaporizing methanol is supplied within the system and, therefore, heating value of liquid methanol is used in efficiency calculations.) Reforming efficiency is calculated as ratio of HHV of hydrogen plus the *net* mechanical work produced by the system (work pro-

Table 8
Flow components and power loads for the methanol reforming system (Case #7)

	ATR air compressor	ATR inlet	ATR exit	H_2 output	Burner air compressor	Burner inlet	Burner exit	Turbine exit
CH_3OH (mol h^{-1})	0	1000	0	0	0	0	0	0
CH_4 (mol h^{-1})	0	0	9.7	0	0	9.7	0	
O_2 (mol h^{-1})	215	215	0	0	1235	1235	712	712
N_2 (mol h^{-1})	808	808	808	0	4646	5454	5454	5454
H_2O (mol h^{-1})	0	1000	732	0	0	641	1476	1476
CO (mol h^{-1})	0	0	283	0	0	192	0	0
CO_2 (mol h^{-1})	0	0	707	0	0	799	1000	1000
H_2 (mol h^{-1})	0	0	2249	1524	0	816	0	0
Total flow (mol h^{-1})	1023	3023	4789	1524	5881	9147	8642	8642
Temperature (°C)	223	218	450		223	324	1149	776
Pressure (atm)	5	5	5	1	5	5	5	1
Heating value (kW)	0.0	212.0	203.0	120.9	0.0	82.2	0.0	0.0
Mechanical work (kW)	−1.66				−9.50			34.39

Table 9
Summary of conversion, power loads and efficiency for the methanol reforming system operating under different sets of optimization parameters

	ATR O:C ratio	H_2 separation (%)	H_2 yield (kW)	Net mechanical work (kW)	H_2 efficiency (%)	Reforming efficiency (%)	Electrical efficiency (%)	T burner exit (C)	T turbine exit (C)
Case 1	0.49	88.6	152.8	21.53	75.8	86.5	47.5	1348	749
Case 2	0.44	89.7	161.4	18.76	80.1	89.4	48.4	1278	706
Case 3	0.44	89.7	161.4	18.91	80.1	89.4	48.5	1149	602
Case 4	0.43	89.7	159.6	19.46	79.2	88.8	48.3	1296	717
Case 5	0.43	89.7	159.6	19.51	79.2	88.8	48.3	1149	599
Case 6	0.43	90.4	160.9	19.05	79.8	89.2	48.4	1149	601
Case 7	0.43	67.8	120.9	23.23	60.0	71.5	40.3	1149	776

duced by the turbine less the load required by all compressors) to the HHV of methanol. Assuming 50% efficiency for a PEM fuel cell and 90% efficiency of a mechanical to electrical generator, electrical efficiency is estimated as the total electrical power that can be produced by the system if coupled with a PEM fuel cell and a generator divided by the HHV of methanol consumed by the system.

Note that while reforming efficiency calculations based on lower heating values (LHV) are often cited in the literature by analogy with combustion systems, a definition based on true energy content, i.e. higher heating value, better accounts for the thermodynamics of the reforming process [10]. Application of LHV does not properly account for the heat required/released in water vaporization/condensation. Therefore, HHV is used as the basis in this analysis.

The results of the system simulations show that methanol system efficiency can be significantly higher than that for the methane reforming system discussed in our previous work [9]. For methane reforming operating at 15 atm system pressure, the overall system efficiency was between 66 and 76% (depending on the set of operating parameter assumptions) with fuel to electricity efficiency between 38 and 41%. For the methanol system discussed here the system efficiency is as high as 89.4% and fuel to electricity efficiency is up to 48.5%. Higher efficiency for the methanol system is due to a lower amount of air required for the ATR reactor, which resulted in a higher H_2 concentration in the reformate stream (almost 50% for methanol versus ~33% for methane) and, hence, a higher separation factor for the membrane separation unit. Also the turbine exhaust stream heat was considered as waste in the methane reforming system while it is used to vaporize water and fuel in the methanol system.

4.2. Effect of ATR temperature

Comparing cases 1 and 2 demonstrates the effect of the ATR operating temperature on the system performance. The difference in the reformate temperature resulted from the difference in the O:C ratio in the ATR inlet stream (0.49 versus 0.44). The higher temperature resulted in lower equilibrium concentration of H_2 and hence lower hydrogen yield from the membrane separator and lower H_2 efficiency (75.8% versus 80.1%). More air was required to burn the CO and H_2 remaining in the membrane retentate stream resulting in the burner exit temperature that was significantly higher than that typically acceptable for turbine materials. In spite of the higher burner air compressor load, more net mechanical work was produced by the system in case 1 than in case 2, but this did not fully compensate for lower hydrogen recovery and thus the overall reforming efficiency was lower for the first system (86.5% versus 89.4%). As noted previously [9], the higher efficiency of mechanical to electrical energy conversion versus that of H_2 to electrical conversion in a PEM fuel cell favors a system with higher mechanical energy produced. Electrical efficiencies of the two systems were nearly equal with only slightly higher efficiency for case 2. Note that a PEM cell efficiency was assumed to be only 50%. At a H_2 production efficiency approaching 90%, the largest increase in the overall fuel-to-electricity efficiency would result from even a marginal increase in the PEM efficiency. Still, taking into account lower burner temperature and lower total gas flow through the system (hence smaller sizes of the turbine and the compressors), there is an advantage for operating the ATR reactor at lower inlet O:C ratios and, therefore, lower reformate temperatures.

4.3. Effect of methane formation

Cases 2 and 4 differ by allowing the formation of 0.2 vol.% CH_4 in the ATR reactor in case 4. This is still much lower than the equilibrium concentration of methane under the specified ATR operating conditions. The methanation reaction is significantly slower than WGS reaction and therefore is kinetically limited. The final methane concentration, thus, was selected to match the previous experimental results [6]. As would be expected, formation of methane lowers the amount of hydrogen in the reformate and, hence, lowers the reforming efficiency. Also, it would be expected that the methanation exotherm would result in a higher reformate temperature leading to higher CO concentrations due to a shift in the WGS equilibrium. However, if the ATR exit temperature is fixed, as it was in our simulations, assuming a feedback control loop adjusting the O:C ratio in the inlet mixture to maintain a constant the ATR exit temperature, then the methane formation reaction results in a lower O:C at the ATR inlet. Methanation also leads to a higher heating value of the membrane retentate stream, which requires a higher amount of air to achieve the specified equivalence ratio (ER = 1.2 in the cases 2 and 4) leading to larger compressor requirements. Also a higher burner exit temperature places more stringent requirements on the turbine blade materials.

4.4. Effect of burner stoichiometry

In an alternative control strategy, the burner exit temperature may be controlled to a fixed level (determined by the turbine material limitations) by adjusting the amount of external air added to the membrane retentate stream before the burner. In cases 3 and 5, which are otherwise identical to the cases 2 and 4, respectively, this second strategy was investigated by controlling the burner exit temperature to 1150 °C. In both cases, almost double the amounts of air flow to the burner was required to limit the temperature, causing a proportional increase in the required compressor work. Higher work was produced by the turbine, however, which offset the compressor work increase such that the system efficiency was essentially unaffected by employing the burner exit temperature control. This result suggests that current turbine designs having air-cooled blades can also be employed without significant loss of system efficiency.

Ability to pass higher air flow through the burner and the turbine without the loss of system efficiency also improves control and stability of the system. ATR operation requires tight control over the O:C ratio at the ATR inlet resulting in broad variations in the ATR air stream in response to variations in ATR exit temperature or to the system power turn down. On the other hand, matching the compressor and the turbine performance requires relatively constant gas flow through the system. When the ATR air makes only a fraction of the overall air flow, such as in cases 3 and 5, variations to this flow would not significantly change the overall system flow and, thus, can be achieved without upsetting the matching properties of the compressor and the turbine.

4.5. Effect of WGS in the membrane

Adding WGS activity to a membrane separator as in the case 6 should convert additional CO into H_2, thus increasing H_2 partial pressure and separation through the membrane. However, our model simulations, as described above, showed that at 80% approach to thermodynamic equilibrium in both membrane segments ($\eta_1 = 0.8$; $\eta_2 = 0.8$) the heat remaining in the retentate stream was insufficient for vaporization of methanol and water at the ATR inlet and the model failed to converge. In order to achieve convergence of the model the membrane separation was decreased to 50 and 52% approach to equilibrium for the first and second membrane segments, respectively ($\eta_1 = 0.5$; $\eta_2 = 0.52$). The results of these case 6 simulations are shown in Table 7. Comparing cases 5 and 6 demonstrates that only slight increase of hydrogen output from the system was achieved (H_2 efficiency increased from 79.2% in case 5 and 79.8% in case 6), while CO concentration in the membrane retentate stream decreased by about a factor of 2. Slightly lower heating value of the retentate stream resulted in lower burner air and, hence, lower compressor work demand. This resulted in the overall system efficiency increase from 88.8 to 89.2%. The fact that only marginal improvements to the system performance result from the addition of WGS activity to the membrane is due, in large part, to the fact that the system is already extremely well integrated thermally. Hydrogen recovery is sufficiently high, and the heat contained in the reformate retentate stream is effectively employed to produce mechanical work in the turbine and to vaporize methanol and water in the heat exchanger such that attempts to further refine the basic process system have only marginal benefit.

Addition of WGS activity to the membrane may provide a significant size advantage to the system, however, by allowing the membrane to operate further from equilibrium separation where higher hydrogen permeation rates could lead to a smaller, less expensive membrane separation unit.

4.6. Effect of system pressure

Operating pressure has a strong effect on membrane separation and on the overall system performance. This effect was studied by lowering the system operating pressure from 15 atm (case 6) to 5 atm (case 7). Note that in order to improve membrane separation at this low pressure, 80% approach to thermodynamic equilibrium was assumed for both membrane segments ($\eta_1 = \eta_2 = 0.8$). (*Note*: unlike the higher pressure case discussed in the preceding section, model convergence could be obtained at $\eta_1 = \eta_2 = 0.8$ for this lower pressure condition). While lower pressure shifts the ATR equilibrium towards hydrogen, such that H_2 concentration in the reformate stream is slightly higher, H_2 separation becomes much lower (decreases from above 90% to only about 69% despite the higher η values employed), burner air requirements increase, and reforming efficiency decreases to 71.5%.

More detailed study of the effect of system pressure on a reformer performance was made in our previous paper [9]. The results of both studies demonstrate very limited effect of pressure on the ATR conversion and selectivity (similarly for conversion of methane and methanol). In both cases, positive effect of higher pressure on membrane separation is dominant with respect to overall system efficiency.

5. Conclusions

The model demonstrates that a compact system for reforming methanol to pure hydrogen can have overall reforming efficiency exceeding 89%. Fuel to electricity efficiency for the system is estimated to be about 48.5% and limited mainly by the efficiency of the PEM fuel cell. The system includes a single boiler/heat exchanger and requires only limited amount of air allowing for a small compressor and compact overall size.

The system performance is improved at low ATR operating temperatures, which are controlled primarily by the air-to-fuel ratio in the inlet stream. This parameter should be optimized in a narrow range where complete methanol conversion is achieved at the lowest possible operating temperature. ATR exit stream temperature can be used to control the amount of air supplied to the ATR.

The ATR catalyst and the operating conditions should be optimized to minimize the methanation reaction. While small amounts of methane formed in ATR do not severely limit the system efficiency, formation of large amounts of methane would lower the efficiency and place additional stress on the compressor and turbine components.

The temperature of the turbine inlet stream can be limited by providing additional air to the inlet of the burner. This does not negatively affect the efficiency and may improve the stability and control of the system.

WGS reaction within a separation unit might result from potential catalytic activity of the Pd-based hydrogen separation membrane. The results indicate that, because of good thermal integration of the system such reaction, were it to occur, would not appreciably benefit the system efficiency. WGS reaction within the separation membrane might lead to reduced size and cost of the separation unit.

The system operation is very sensitive to the operating pressure. When system pressure decreases from 15 to 5 atm the efficiency decreases from ∼89 to ∼71% in spite of more stringent assumptions on the membrane performance at low pressure.

References

[1] N. Takezawa, N. Iwasa, Catal. Today 36 (1997) 45–56.
[2] P.J. de Wild, M.J.F.M. Verhaak, Catal. Today 60 (2000) 3–10.
[3] A. Karim, J. Bravo, D. Gorm, T. Conant, A. Datye, Catal. Today 110 (2005) 86–91.
[4] S. Velu, K. Suzuki, M. Okazaki, M.P. Kapoor, T. Osaki, F. Ohashi, J. Catal. 194 (2000) 373–384.
[5] J. Kugai, S. Velu, C. Song, Catal. Lett. 101 (2005) 255–264.
[6] M. Lyubovsky, S. Roychoudhury, Appl. Catal. B: Environ. 54 (2004) 203–215.
[7] G.A. Deluga, J.R. Salge, L.D. Schmidt, X.E. Verykios, Science 303 (2004) 993–997.
[8] J.R. Lattner, M.P. Harold, Appl. Catal. B: Environ. 56 (2005) 149–169.
[9] M. Lyubovsky, D. Walsh, J. Power Sources 157 (2006) 430–437.
[10] Ulf Bossel, Well-to-Wheel Studies, Heating Values, and the Energy Conservation Principle European Fuel Cell Forum, 29 Octorber 2003. http://www.efcf.com/reports/E10.pdf.